General Disclaimer

One or more of the Following Statements may affect this Document

- This document has been reproduced from the best copy furnished by the organizational source. It is being released in the interest of making available as much information as possible.

- This document may contain data, which exceeds the sheet parameters. It was furnished in this condition by the organizational source and is the best copy available.

- This document may contain tone-on-tone or color graphs, charts and/or pictures, which have been reproduced in black and white.

- This document is paginated as submitted by the original source.

- Portions of this document are not fully legible due to the historical nature of some of the material. However, it is the best reproduction available from the original submission.

NASA TM X-73511

NONPROPULSIVE APPLICATIONS OF ION BEAMS

by W. R. Hudson
Lewis Research Center
Cleveland, Ohio 44135

NONPROPULSIVE APPLICATIONS OF ION BEAMS

W. R. Hudson
National Aeronautics and Space Administration
Lewis Research Center
Cleveland, Ohio 44135

Abstract

This paper describes the results of an investigation of the nonpropulsive applications of electric propulsion technology. Eight centimeter ion beam sources utilizing xenon and argon have been developed that operate over a wide range of beam energies and currents. Three types of processes have been studied - sputter deposition, ion beam machining, and ion beam surface texturing. The broad range of source operating conditions allows optimum sputter deposition of various materials. An ion beam source has also been used to ion mill laser reflection holograms using photoresist patterns on silicon. Ion beam texturing has been tried with many materials and has a multitude of potential applications.

Introduction

Nonpropulsive applications of electric propulsion technology have been under investigation at the Lewis Research Center for the past eighteen months. This program is a spinoff from 15 years of research and development of electron bombardment mercury ion thrusters for primary propulsion and satellite stationkeeping applications. The program has been involved with both the adaption of thruster technology to ion beam source technology and the exploration of a wide range of potential applications.

All of the experiments described in this paper were performed with a xenon source that is patterned after the eight centimeter mercury ion thruster. Ion beam sources similar to the sources described herein are presently commercially available[1,2] These sources are commonly used for cleaning silicon substrates preparatory to integrated circuit fabrication for ion-milling photoresist patterns in the fabrication of microelectronic, microwave acoustic, and integrated optics components.[3] Similarly, high density microstructure arrays of permalloy magnetic dipoles have been ion-milled for magnetic bubble devices.[4] Much higher resolution can be achieved with ion-milling than with chemical etching. Patterns with line widths of 1000 Å have been obtained and contamination from chemical etching is avoided. Other applications include preparing clean surfaces for surface science research,[5] polishing of copper surfaces for laser mirrors[6] and producing aspheric lenses.[7] A complete bibliography of ion beam technology is presented in reference 8.

The results of experiments encompassing a wide range of potential applications are reported in this paper. Three types of ion beam sputtering processes have been studied: sputter deposition, ion beam machining and ion beam surface texturing. Figure 1 shows how the processes have been categorized on the basis of the relative positions of the source, target and substrate. In sputter deposition, (fig. 1a) the most obvious applications, the ion beam impinges on the target material to be sputter deposited. The energetic ions strike the target surface causing the ejection of target ma-

terial, which is then deposited onto a substrate. In ion beam machining (fig. 1b) a mask is placed between the source and the target, such that target material is selectively removed from the unshielded locations. Figure 1(c) shows the arrangement of the source, target, and seed material used for ion beam surface texturing. The material to be textured is located in the target position and can be oriented at any angle with respect to the ion beam. A low sputtering yield seed material is mounted on a separate support and typically oriented at a forth-five degree angle with respect to the beam. The seed material also is located within the beam envelope very close to but not touching the target. The ion beam simultaneously sputters both the target and the seed material creating a microscopic surface structure on the target.

The work described in this paper is divided into four sections. The first section described the ion beam source and the sputtering facility. The other three sections cover the ion beam processes described in the preceding paragraph.

Ion Beam Sources and Sputtering Facilities

An eight centimeter-diameter beam xenon source, (fig. 2), was used for all the applications reported on in this paper. The source had enclosed keeper hollow cathodes[7] with barium oxide-impregnated porous tungsten inserts for both the main cathode and the neutralizer. The magnetic circuit had a cusped field geometry[8] with permanent rod magnets around the perimeter of the discharge chamber. The optics for beam extraction consisted of dished double grids with a small hole accelerator grid.[11]

Figure 3 is a sketch of the ion beam source facility. The xenon source is mounted on a flange which in turn mounts onto one of the ports of a large vacuum facility. The port is connected to the main tank by a 0.91-meter diameter gate valve. The vacuum facility has three 0.75-meter diameter diffusion pumps. The facility can be evacuated to 10^{-7} torr and with ion beam source on operates at 2×10^{-5} torr. The source is mounted on tracks so that it can be displaced along a line parallel to its axis. Sputtering targets are mounted on "shepherds' crook" supports, that can either be rotated or displaced parallel to the source axis. The targets can be mounted with their surface at any angle with respect to the ion beam. It is possible to mount multiple targets and interchange them by rotating the target support. Substrates and measuring devices can be introduced to the test facility through five centimeter and ten centimeter diameter sideports. This separate entry capability allowed samples to be removed for inspection or replaced without turning off the source and exposing it to air. It also greatly reduced the turn around time. The substrates were supported by a rod which could be translated perpendicular to the ion beam and rotated around the rod axis. Viewing ports allowed viewing of the targets and substrates for positioning, as well as temperature measurements by optical pyrometry.

Electric propulsion technology has enabled the development of xenon ion beam sources capable of operation over a broad range of ion accelerating voltage and ion beam current. The xenon source can be operated at beam currents between 10 and 200 mA. The net accelerating potential, V_I, can be varied from 300 to 2000 V. At positions five and ten centimeters downstream from the source the ion beam uniformity is ±10% over a four centimeter diameter in the center of the beam. The capability of varying both the net accelerating voltage and the beam current is essential. For some materials it is necessary to reduce the beam energy to prevent damaging the target by overheating. For low sputtering yield materials the maximum beam energy is desirable for obtaining useful sputter deposition rates.

Ion beam sputtering has several useful characteristics in addition to a broad range of ion beam energies. The freedom to vary the angle of incidence of the beam with respect to the target maximizes sputter yield. The low facility pressure decreases gas inclusions in deposits and minimizes backsputtering. The deposition environment may be separated from the sputter source and the substrate temperature may be controlled. There is also considerable electrical flexibility in that targets and substrates may be grounded, isolated or arbitrarily voltage biased.

As part of the applications program at Lewis Research Center, an effort has been made to develop a low-cost argon source. The choice of an argon source is dictated primarily by source gas cost. Xenon is currently two hundred and forty times more expensive than argon. The xenon source operating on an average of eighty hours per week requires one hundred dollars (1976 dollars) of xenon. It is also desirable to develop a source that is easily operated, durable, and simple to maintain. A useful source for general application should not require an expert operator. The electronic power supplies should have a minimum of controls and require a minimum of tuning while having sufficient flexibility so as not to sacrifice utility. Parametric studies of hollow cathode operation with argon indicate that for small sources (15 cm diameter and less) and beam currents less than 500 mA, it is better to use thermionic emitters. Furthermore, thermionic emitters are simpler to fabricate and operate. Their short operating lifes are not a major drawback for ground based applications. Another area for optimization is beam flatness. It is presently thought that this can be achieved by increasing the source diameter and by converting to a multipole discharge chamber design.

Ion Beam Sputter Deposition

Table I is a list of the materials that have been ion beam sputter deposited. The xenon source described earlier was used, with the target and substrate positioned as indicated in figure 1(a). In all cases the 7.5-cm diameter target was oriented at an angle of 45° with respect to the axis of the source. The table also includes the ion source operating conditions for each rate. The sputter deposition rates were measured with a quartz crystal microbalance located in the substrate position.

Several different kinds of material were sputter deposited: metals, semiconductors, insulators, and polymers. Different ion source operating con-

ditions were required because of differences in the thermal properties of the target materials. For example, teflon must be sputtered at low ion beam power to minimize thermal fracturing of the polymer, whereas carbon can be subjected to the maximum beam energy of the source without damage. Because the sputtering yield of carbon is low, the higher beam energy is necessary to achieve useful sputter deposition rates.

It has generally been found to be very useful to thoroughly clean ion beam sputter substrates prior to initiating deposition. One unique advantage of ion beam sputtering is that it is possible to go continuously from substrate etching to deposition. This procedure together with the high velocity of the sputtered atoms results in very good adherence of the deposition film. For metals and polymers adherent coatings were achieved with no substrate heating. To obtain adherent films of SiO_2 and Al_2O_3 required that the substrate be heated to approximately 400° C.

Silicon Films

Several specific sputter deposition projects were undertaken. One of the first projects was the deposition of silicon. Thin film silicon deposits are currently of great interest for terrestrial solar energy applications. If high quality silicon films could be deposited over large areas at a reasonable cost it would be a technological breakthrough. The basic problem is to deposit films of sufficiently large crystallite size such that electrons can be collected with reasonable efficiencies before they become neutralized at grain boundaries. Several different substrate positions and orientations were tested with quartz, sapphire, and single crystal silicon as substrates. The substrates were heated during deposition to 1000° C. The purpose of heating the substrate was to increase the surface mobility of the silicon and thereby enhance crystal growth and increase crystallite size. The crystal orientation and grain size were analyzed with an x-ray Bragg diffractometer. The deposits were all observed to have a 110 orientation, indicating no epitaxial growth occurred on any of the substrates. The maximum crystallite size was 1000 Å on the sapphire substrate.

Fabrication of Thin Film Capacitors

The recent miniaturization of electronics that has resulted from integrated circuit technology has created a need for small lightweight auxiliary components such as capacitors. Thin film capacitors, particularly multiple layer capacitors, [12] have the potential for filling this need.

Initially SiO_2 and Al_2O_3 were deposited for the insulating layer, but after some preliminary tests teflon proved to be a superior material, primarily because teflon is much more convenient to deposit. Achieving good adherence with SiO_2 or Al_2O_3 requires the substrate to be heated to 400° C while teflon films can be deposited on substrate at room temperature. Single layer teflon capacitors have been fabricated by Miller and Ruff [13] using R. F. sputtering.

Considerable care is required to successfully fabricate thin film capacitors. A very thorough cleaning procedure is required, because any surface contaminant or surface feature can potentially short

out the capacitor. A dust free environment is essential. Substrates must be free of scratches and pits. Single layer capacitors, like the one shown in figure 4, are made by sequential deposition of an aluminum film, a teflon film, and then another aluminum film. Masks are used to define the film deposition boundaries. A 1-millimeter clearance was intentionally left between the mask and the substrate for two reasons. First some space is required so that mask can be removed without damaging previously deposited films, but more importantly it also results in a tapered film edge. Tapered film edges allow deposition of layer films without developing shorts at the edges.

Table II is a comparison between bulk teflon, R. F. sputtered teflon and ion beam sputtered teflon. The films are very similar. Figure 5 shows the dependence of capacitance on teflon thickness deposited by ion beam sputtering. The measured capacitance agrees reasonably well with the inverse thickness dependency predicted by the simple capacitor equation

$$C = \frac{K\epsilon_o A}{d}$$

where K is the dielectric constant, ϵ_o is the permittivity of free space, A is the active area, and d is the thickness.

The current emphasis of the thin film capacitor program is on the investigation of problems associated with depositing multiple layers on low cost, thin glass substrates. A remotely operated mask changer has been developed which makes it possible to precisely change masks without removing the capacitor from the vacuum system. This in situ operation eliminates contamination from dust or handling.

General Purpose Deposition

Teflon films have applications in many areas other than capacitor fabrication, such as lubrication and corrosion applications. One particularly unique example is the encapsulation of pressure transducers that are implanted in the human body. The body fliuds offer an extremely corrosive environment and the long term protection of implanted devices is a major biomedical problem.

Ion beam sputter deposition is particularly well suited for depositing carbon. Because carbon has one of the lowest sputtering yields it is difficult to deposit at high rates. With a beam current of 150 mA, a net accelerating voltage of 2000 volts, and with the target oriented at 45° with respect to the beam, adherent coatings have been achieved at rates of 300 Å/min. Since the carbon target was well below its melting point, much higher rates are possible with higher beam currents. Even further increase of sputtering rates is possible if the target is cooled.

It is also possible to create composite films by sputtering targets composed of more than one material. The sputter deposits that result will be homogenous mixtures of the target materials. Any combination of solid materials is theoretically possible. Such combinations as aluminum-copper and teflon-copper have been deposited. This technique can create a whole new class of materials, some of which may have interesting and useful properties.

The relative ratio of constituents is determined by the target area struck by the ion beam and the relative ratio of the sputtering yields.

Ion Beam Machining

Ion beam machining as used herein refers to erosion processes where the workpiece is immersed directly in the ion beam. Some examples of processes that are presently well established include ion beam cleaning of silicon, ion beam milling of integrated optical electronics components, and ion beam milling of diffraction gratings. In the sections that follow some specific applications of ion beam machining are discussed.

Ion Beam Polishing

Seven metal samples-aluminum, copper, brass, tantalum, iron, galvanized and stainless steel were first sand blasted to obtain a uniform well defined roughness and then polished with an ion beam. The sandblasting conditions were as follows: 50µ SiC grit, 65 N/cm^2 (80 psig) pressure, with the nozzle oriented perpendicular to the metal surface and positioned 2 5 cm away. The samples were then cut in half, one half was retained for documenting the initial surface roughness and the other half was ion beam polished. The seven samples were mounted such that the ion beam was directed tangential to the sample surface. The beam preferentially sputters the high points thus polishing the surface. The samples were polished in this manner for twenty-four hours at a net accelerating voltage of 1000 volts and a beam current of 100 mA. After polishing the samples were then examined using a scanning electron microscope. Photomicrographs of brass and tantalum surfaces before and after polishing are shown in figure 6. Two results were immediately apparent. First, not surprisingly, the softer materials were more readily polished and, second, the polished surfaces appeared channeled or grooved. The appearance of grooves strongly suggests the need for rotating the sample during polishing.

Ion Beam Drilling

Figure 7 is a photograph of a carbon mask covering a 1.6 mm thick stainless steel backing sheet that were used for ion beam drilling of irregularly shaped holes. The ion beam was directed perpendicular to the surface of the mask. Because stainless steel sputters at a much faster rate than carbon, holes can be drilled in the stainless backing sheet with very little change in the mask thickness. The experiment operated for 75 hours at a net accelerating voltage of 1000 volts and a beam current of 100 mA. The holes that resulted were uniform in size across the thickness of the target and a very exact reproduction of the mask openings. The etching rate of the stainless steel was 2100 Å/min which produced holes 0.9-mm deep as shown in figure 7. Ion beam drilling is especially applicable for producing arrays of irregularly shaped holes.

Ion Beam Milling

Laser reflection holograms have also been fabricated by ion beam milling. Photoresist patterns are first printed on the silicon work piece and then sputtered with an ion beam. Material is selectively sputtered away in regions where the workpiece is not covered by photoresist. After sputtering to the desired depth, the remaining photoresist is chemically

3

removed. Figure 8 is a photograph of a hologram that was milled at a distance of 20 cm and 300 volts net accelerating voltage at 10 milliamperes of beam current. The low ion beam energy was required because of the relatively low temperature melting point of the photoresist material. Figure 9 shows two scanning electron photomicrographs at 100 X and 1000 X. This hologram was subsequently tested using a helium-neon laser and produced a satisfactory image. The primary advantages of ion beam milling holograms are the accurate reproduction of the photoresist patterns and the avoidance of chemical contamination and undercutting.

Ion Beam Texturing

Background

In 1942 Guentherschulze and Tollmien[14] observed angular variations in the surface reflectivity of flow discharge cathodes that they hypothesized were the result of a submicroscopic surface texture. Later Stewart and Thompson[15] published scanning electron photomicrographs of conical protrusions on tin and silicon surfaces that had been sputter etched with a radio-frequency argon ion source. They concurred with Guentherschulze's postulation that the cones occur where low sputtering yield particles protect the underlying material from sputtering. Wehner and Hajicek[16] have shown that surface texture can be produced by supplying surfaces with lower sputtering yield atoms (seed material) during sputter etching. It is thought that the low sputtering yield atoms agglomerate into microscopic regions, thus preventing the higher sputtering yield atoms beneath them from being sputtered. This paper presents results of ion beam texturing of surfaces for a number of elements and compounds. Scanning electron photomicrographs are presented which show the resulting surface texture characteristic of different regions of the periodic table. Photomicrographs are also presented which document the initial stages and growth of the surface texture. Variations of the texture with seeding material, ion energy, beam current and surface temperature have been studied.

Ion Beam Texturing Process

For ion beam texturing the ion source was operated at a net accelerating potential of 1000 volts and a beam current of 100 mA. The current density at the center of the beam ten centimeters from the source was 2.0 mA/cm^2. The specific operating conditions were varied depending on the melting point of the target material.

The material to be textured was located 10-centimeters from the source and centered in the ion beam. Although it could have been oriented at any angle, it was mounted with the ion source axis normal to its surface. The seed material was mounted on a separate support and was oriented at a $45°$ angle with respect to source axis. The ion beam simultaneously sputtered both the target and the seed material. Sufficient seed material was sputter deposited onto the target such that a dense uniform texture was created over areas up to three centimeters in diameter.

Morphology of Textured Elements

Ion beam texturing using tantalum as the seed material was attempted on thirty different elements. Twenty-six elements were successfully textured and are shown shaded in figure 10. The texturing process was unsuccessful for Nb, Mo, Ta and W, the four crosshatched elements in figure 10. All of the elements that could not be textured are in columns VB and VIB of the periodic chart. It is interesting to compare this observation with the periodicity effect of the low energy sputtering yield (fig. 11) that has been reported by Wehner[17] and by Wehner and Rosenberg.[18] The elements (Nb, Mo, Ta, W) that showed no signs of texture are all relatively low sputtering yield materials. However, several elements (C, Si, Ti, and Zr) have lower sputtering yields than tantalum, but nevertheless were still textured. Conversely, tungsten has a higher sputtering yield than tantalum but did not texture. The elements in column IVB of the periodic chart all could be textured; however zirconium textured at a faster rate (4.3×10^{-6} cm/min) than either hafnium (6.7×10^{-7} cm/min) or titanium (1.0×10^{-6} cm/min).

It is extremely difficult to describe the morphological differences of the twenty-six elements that were textured. A large number of elements had textures that can be classified as either a ridge structures or a cone structures. Figure 12(a) is a photomicrograph of the convoluted ridge morphology that occurred with nickel and many of the other low sputtering yield materials (Ti, Fe, Co, Zr, Hf, Gd). Many of the higher sputtering yield materials had morphologies that look like densely packed cones or needles. The scanning electron photomicrograph of copper shown in figure 12(b) is an example of the cone structure. The other elements that exhibit this type of structure include Mg, Cr, Ag, Au, Hg, Al, C, Si, Ge, Pb and Bi. The remaining materials that textured but showed neigher a ridge structure nor a cone structure are C, Be, Zn, Dn, Sn, and Sb. Their surface textures were all unique. Analysis of the x-ray energy dispersion of textured silicon confirmed Wehner's postulation that the regions on the top of the cones had considerably more tantalum than the regions between the cones.

In addition to the elements, a few compounds, alloys and polymers such as stainless steel, CrAu, and teflon have been textured. The resulting surface morphologies were also identifiable as ridge and cone structures.

The Evolution of Surface Texture

A series of copper samples were ion beam textured at a net accelerating voltage of 1000 volts and a beam current of 100 mA for periods of two, four, eight, sixteen, and thirty-two minutes. Figure 13 shows two scanning electron microscope views of the two minute textured surface. The vertical view shows the distribution of what are believed to be the tantalum nucleation sites. They seem to be composed of islands 0.1 to 0.5 μm in diameter. The angular view shows the depth of the structure and the initiation of the texture. Figure 14 shows the surface texture after four minutes of ion beam texturing. The peaks are on the average somewhat larger in diameter than after two minutes and in a few locations appear to be lined up in rows. After four minutes the formation of the cone structure is clearly well underway. After eight minutes the surface is completely textured and looked almost exactly like figure 10(b). Further exposure to the ion beam only resulted in increased depth of the structure. Note that some of the cones in fig-

ure 10(b) appear to be hollow. The necessity of continually supplying seed material was demonstrated by the following test. A copper surface was first textured with a 100 mA, 1000 volt ion beam for thirty minutes after which the tantalum seed material was rotated out of the ion beam and the surface was sputter etched for one minute at the same beam current and voltage. The cone structure was almost completely removed.

Measurements of the average copper cone height with respect to the ion beam exposure time are graphed in figure 15. The curve has a change in slope between the four minute point and the eight minute point. This is probably a result of the transition from the initial stages of texturing to the lower sputtering yield later stages where more sputtered atoms are trapped by the cones. The cone growth rate in the later stage is estimated at 0.09 μm/min. At the same beam conditions the copper etch rate with no tantalum present was 0.12 μm/min. By way of comparison stainless steel has a texture growth rate of 0.01 μm/min under the same conditions.

Texturing Parameters

There are several parameters which influence the texturing process, such as the kind of seed material, its arrival rate at the target, the net accelerating voltage, the beam current, and the target temperature. A complete analysis of the large number of parametric perturbations is beyond the scope of this paper, nevertheless some specific observations are of interest.

Figure 16 shows textured copper surfaces that resulted with tungsten as seed material and with Al_2O_3 as seed material. The morphologies were different from each other and different from those created with a tantalum seed material, figure 12(b). However, a different seed material does not always result in a different morphology. When silicon was textured with tantalum, molybdenum, or titanium the resulting morphologies were found to be nearly identical.

The structure density of the texture (the number of cones or ridges per unit area) was found to be dependent on the arrival rate of the seed material. At low arrival rates the cones were more widely separated and more perfectly formed. It is also possible for the seed material arrival rate to be so high that no texture forms on the target.

Preliminary measurements of the growth rate of stainless steel texture found it to be proportional to both beam current and net accelerating potential.

Surface temperature is also very important to the texturing phenomena. For example if the normal texturing process of copper with tantalum seed material was interrupted after every minute of operation and allowed to cool for several minutes, no texture was created. Instead the copper became coated with tantalum. This may have resulted because of the temperature activated surface mobility of the seed material as postulated by Wehner.

Concluding Remarks

An existing 8-cm xenon ion thruster was adapted to serve as the ion beam source for a investigation into non-propulsive applications. The ion beam source has proven to be very useful for general purpose sputter deposition. Several materials that are difficult to sputter by other techniques such as Al_2O_3, SiO_2, carbon, and teflon can be sputter deposited at useful rates using this ion beam. Encouraging results have been obtained in the construction of thin film teflon capacitors. Preliminary measurements of the thickness dependence of the capacitance and the dielectric field strength have been made.

Other experiments on ion beam machining processes - polishing, drilling, and milling have been successful. Several metallic surfaces have been ion beam polished with good results. The polishing could be further improved by rotating the sample. Laser reflection holograms have been ion beam milled and preliminary experiments have demonstrated very accurate reproduction of the photoresist patterns.

An ion beam source has demonstrated the ability to produce a controlled texturing of surfaces. Twenty-six elements have been textured and the resulting surface morphologies have been characterized. A large number of elements had textures that could be classified as either a ridge structure of a cone structure.

The surface morphology created by ion beam texturing has different areas of potential applications. This type of surface treatment could be used to modify reflectance and emissivity, to decrease secondary electron emission, to promote thin film adhesion, to increase catalytic reactions, and to reduce the effective sputtering yield.

References

1. Laznovsky, W., "Advances in Low-Energy Ion Beam Technology." Research/Development, Vol. 26, Aug. 1975, pp. 47-55.

2. Reader, P. D., Kaufman, H. R., "Optimization of an Electron-Bombardment Ion Source for Ion Machining Applications," presented at the 13th Ion Beam Technology Symposium, Colorado Springs, Colorado, May 1975.

3. Garvin, H. L., "High Resolution Fabrication by Ion Beam Sputtering," Solid State Technology, Vol. 16, Nov. 1973, pp. 3-136.

4. Spencer, E. G., Schmidt, P. H., and Fisher, R. F., "Microstructure Arrays Produced by Ion Milling," Applied Physics Letters, Vol. 17, Oct. 1970, pp. 328-334.

5. Farnsworth, H. E., et al., "Application of the Ion Bombardment Creaming Method to Titanium, Geranium, Silicon, and Nickel as Determined by Low-Energy Electron Defraction," Journal of Applied Physics, Vol. 29, Aug. 1958, pp. 1150-1161.

6. Hoffman, R. A., Lange, W. J., and Choyke, W. J., "Ion Polishing of Copper: Some Observations," Applied Optics, Vol. 14, Aug. 1975, pp. 1803-1807.

7. Yasuda, H., "Figuration of Wedge-Shaped and Parabolic Surfaces by Ion Etching," Japanese Journal of Applied Physics, Vol. 12, Aug. 1973, pp. 1139-1142.

8. Hawkins, D. T., "Ion Milling (Ion-Beam Etching), 1954-1975: Journal of Vacuum Science Technology., Vol. 12, Nov/Dec. 1975, pp. 1389-1398.

9. Hudson, W. R. and Weigand, A. J., "Hollow Cathodes with BaO Impregnated, Porous Tungsten Inserts and Tips," AIAA Paper 73-1142, Lake Tahoe, Nev., Oct.-Nov. 1973.

10. Beattie, J. R. and Wilbur, P. J., "15 Cm Cusped Magnetic Field Mercury Ion Thruster Research," AIAA Paper 75-429, New Orleans, La., Mar. 1975.

11. Hudson, W. R., "Auxiliary Propulsion Thruster Performance with Ion Machined Accelerator Grids," AIAA Paper 75-425, New Orleans, La., Mar. 1975.

12. Maissel, L. and Glang, R., Handbook of Thin Film Technology, McGraw-Hill, 1970.

13. Miller, R. I., and Ruff, R. C., "Effects of Sputtering Parameters on Teflon Thin Film Capacitors," NASA TM X-53937, June 1970.

14. Guentheschulse, A., and Tollmien, W., "Neue Untersuchungen uber die Kathodenzerstaubung der Glimmenttadung," Zeitschrift fuer Physik, Vol. 119, 1942, pp. 685-695.

15. Stewart, A. D. G., and Thompson, M. W., "Microtopography of Surfaces Eroded by Ion-Bombardment," Journal Material Sciences, Vol. 4, Jan. 1969, pp. 56-60.

16. Wehner, G. K., and Hajicek, D. J., "Cone Formation of Metal Targets During Sputtering," Journal of Applied Physics, Vol. 42, Mar. 1971, pp. 1145-1149.

17. Wehner, G. K., Proceedings of the 5th International Conference on Ionization Phenomena in Gases, Vol. II, H. Maecker, ed., North-Holland Publ. Co. (Amsterdam), 1962, pp. 1141-1156.

18. Wehner, G. K., and Rosenberg, D., "Mercury Ion Beam Sputtering of Metals at Energies 4-15 keV," Journal of Applied Physics, Vol. 32, May 1961, pp. 887-890.

TABLE I. - Sputter Deposition Rates

(produced with Xenon Sputtering Source)

Material	Deposition rates, A/min	Beam intensity,	
		kV	mA
Aluminum	1460	1	150
Copper	1930	1	150
Carbon	300	2	150
Gold	1130	1	150
Silicon	1170	2	185
Molybdenum	585	1	165
Teflon*	250	1	50
Aluminum Oxide Al_2O_3	250	2	190
Quartz SiO_2	950	2	190

*Trademark

TABLE II. - Teflon Properties

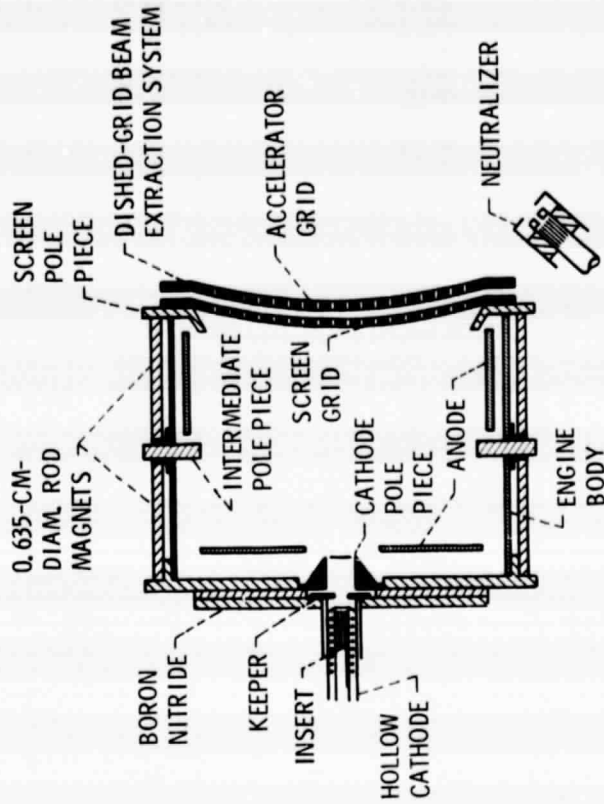| Property	Bulk value	R.F. Sputtered films	Ion beam sputter films
Dissipation factor, D.F.	2×10^{-4}	$5 \times 10^{-3} - 5 \times 10^{-2}$	$2 \times 10^{-3} - 8 \times 10^{-3}$
Resistivity, ρ	1.9×10^{19} Ωcm	$10^{13} - 10^{15}$ Ωcm	10^{12} Ωcm
Dielectric strength, $\overline{VV}_{B.D.}$	1.57×10^5 V/cm	$2 \times 10^5 - 5 \times 10^6$ V/cm	1×10^6 V/cm
Dielectric constant, K	2.1	1.4 - 7.4	1.4 - 6.8

Figure 2. - Cross section of 8-centimeter diameter source discharge chamber with cusp magnetic field and dished-grid beam extraction system.

(a) ION BEAM SPUTTER DEPOSITION.

(b) ION BEAM MACHINING.

(c) ION BEAM SURFACE TEXTURING.

Figure 1. - Sketch categorizing ion beam processes.
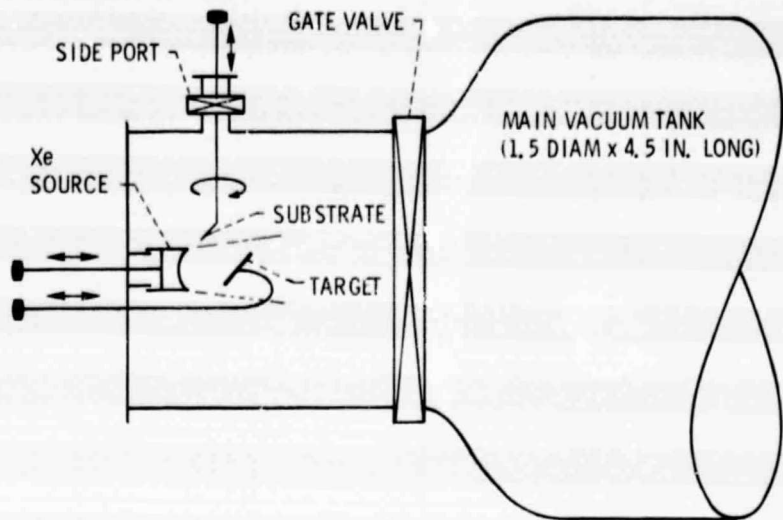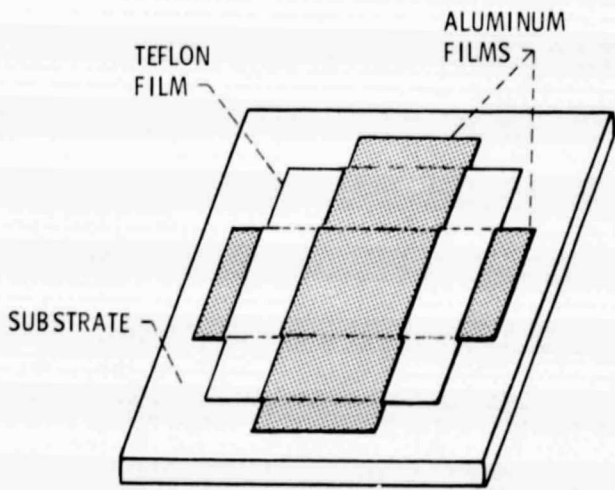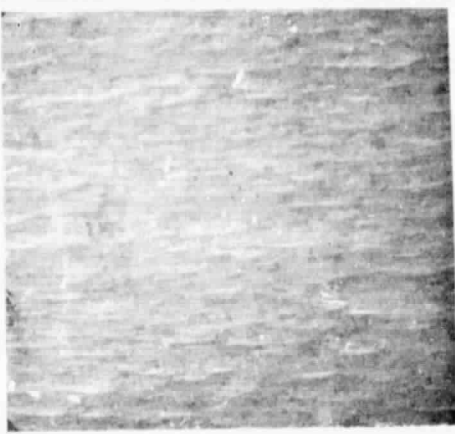
Figure 3. - Sketch of ion source facility showing operational arrangement.

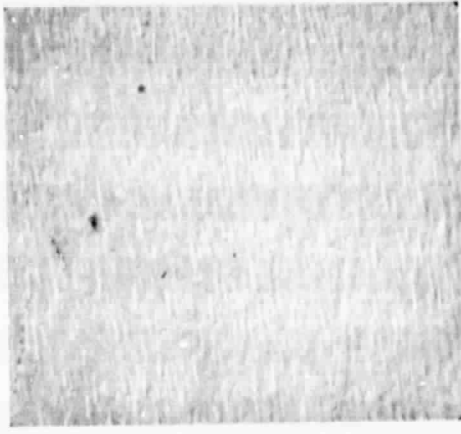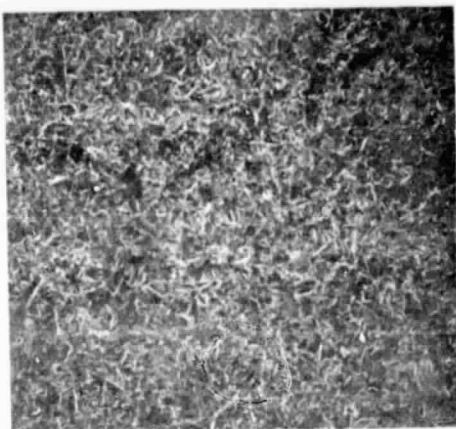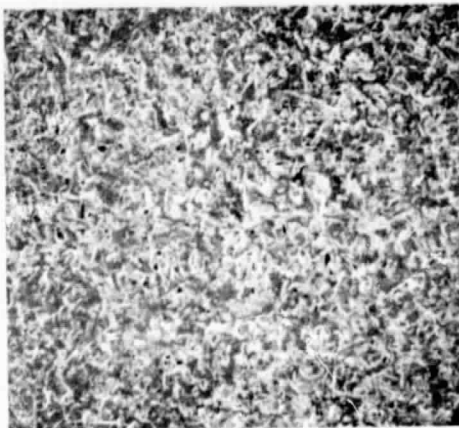Figure 4. - Sketch of thin film teflon capacitor.

ION POLISHED BRASS

ION POLISHED TANTALUM

GRIT BLASTED BRASS

GRIT BLASTED TANTALUM

100 μm

Figure 6. – Scanning electron microscope photomicrographs of brass and tantalum before and after ion polishing.
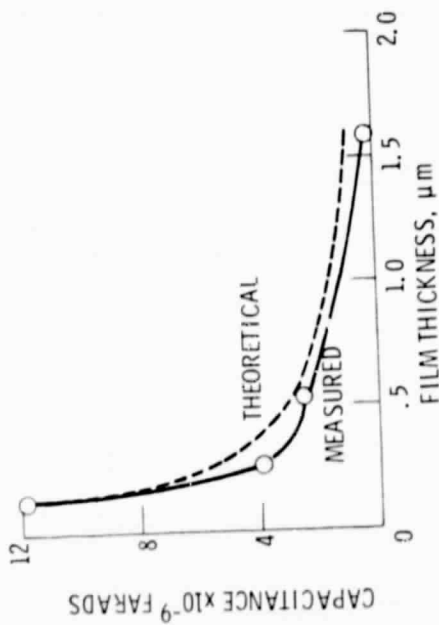
Figure 5. – Measured capacitance as a function of thickness, the dashed line is an inverse thickness dependence.
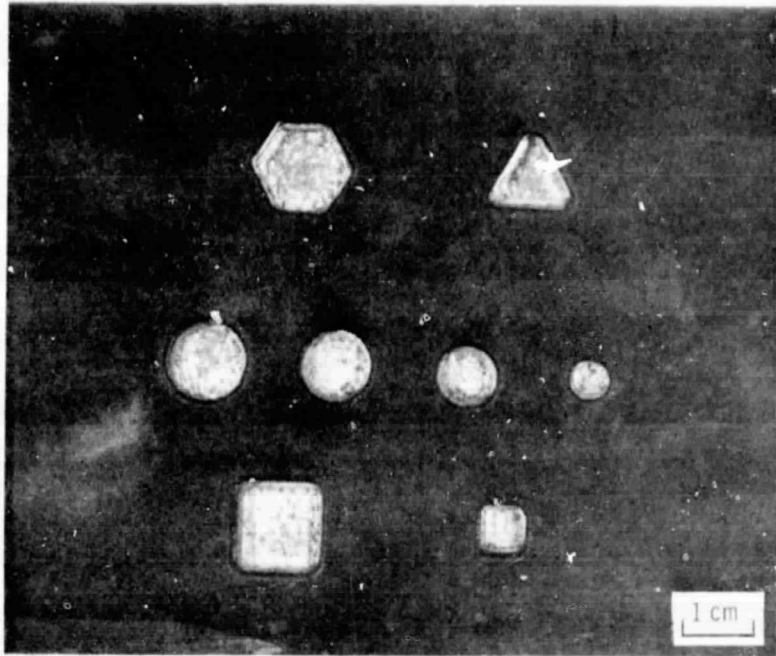
THEORETICAL

MEASURED

CAPACITANCE x10^{-9} FARADS

FILM THICKNESS, μm

Figure 7. - Carbon mask covering a stainless steel sheet that has been
exposed to ion beam for 75 hours. Net accelerating voltage, 1000 volts;
beam current, 100 ma. Holes are 0.9 mm deep in stainless steel sheet.
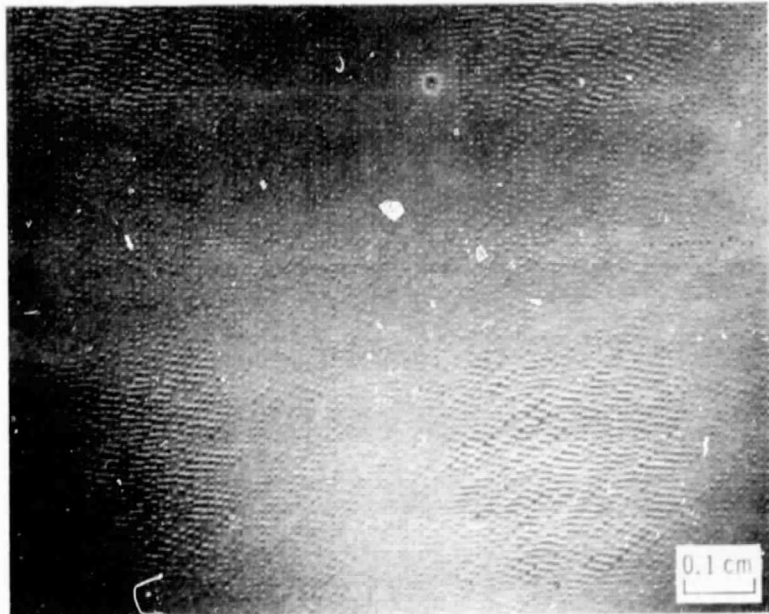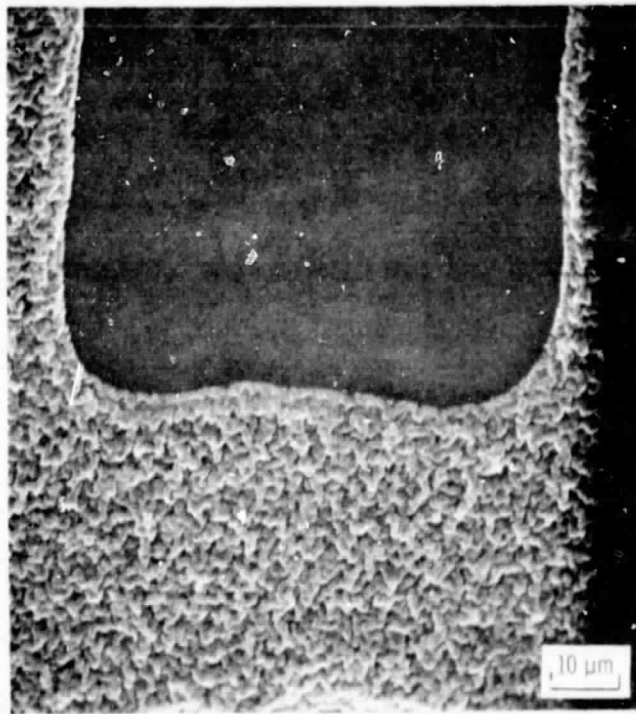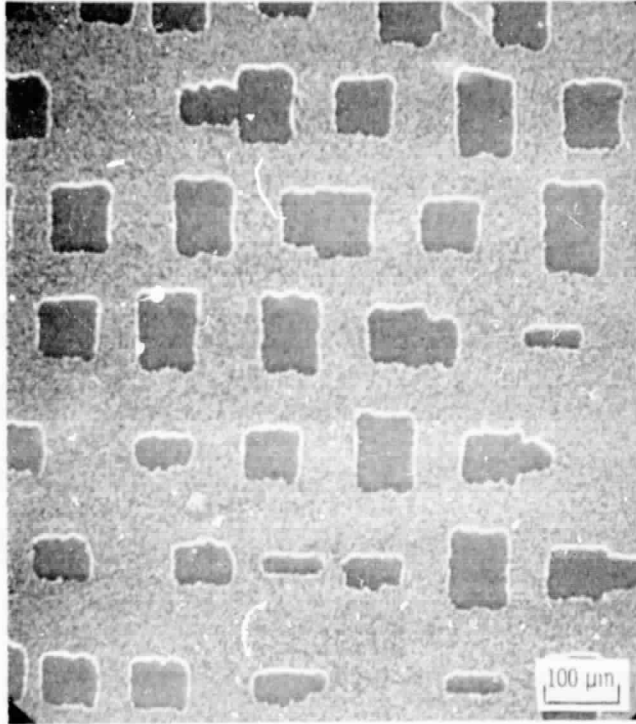Carbon mask, 0.5 mm thick.

Figure 8. - Ion milled laser hologram. X10.

Figure 9. - Scanning electron photomicrographs of an
ion beam milled reflection hologram.

PERIODIC CHART OF THE ELEMENTS

E-8851

IA	IIA	IIIB	IVB	VB	VIB	VIIB	VIII			IB	IIB	IIIA	IVA	VA	VIA	VIIA	INERT GASES
1 H																	2 He
3 Li	4 Be											5 B	6 C	7 N	8 O	9 F	10 Ne
11 Na	12 Mg											13 Al	14 Si	15 P	16 S	17 Cl	18 A
19 K	20 Ca	21 Sc	22 Ti	23 V	24 Cr	25 Mn	26 Fe	27 Co	28 Ni	29 Cu	30 Zn	31 Ga	32 Ge	33 As	34 Se	35 Br	36 Kr
37 Rb	38 Sr	39 Y	40 Zr	41 Nb	42 Mo	43 Tc	44 Ru	45 Rh	46 Pd	47 Ag	48 Cd	49 In	50 Sn	51 Sb	52 Te	53 I	54 Xe
55 Cs	56 Ba	57 La	72 Hf	73 Ta	74 W	75 Re	76 Os	77 Ir	78 Pt	79 Au	80 Hg	81 Tl	82 Pb	83 Bi	84 Po	85 At	86 Rn
87 Fr	88 Ra	89 Ac															

*LANTHANUM SERIES

58 Ce	59 Pr	60 Nd	61 Pm	62 Sm	63 Eu	64 Gd	65 Tb	66 Dy	67 Ho	68 Er	69 Tm	70 Yb	71 Lu

†ACTINIUM SERIES

90 Th	91 Pa	92 U	93 Np	94 Pu	95 Am	96 Cm	97 Bk	98 Cf	99 E	100 Fm	101 Mv

Figure 10. - The periodic chart of the elements. The shaded elements were successfully textured using tantalum as the seed material. The texturing process was unsuccessful for the cross-hatched materials.
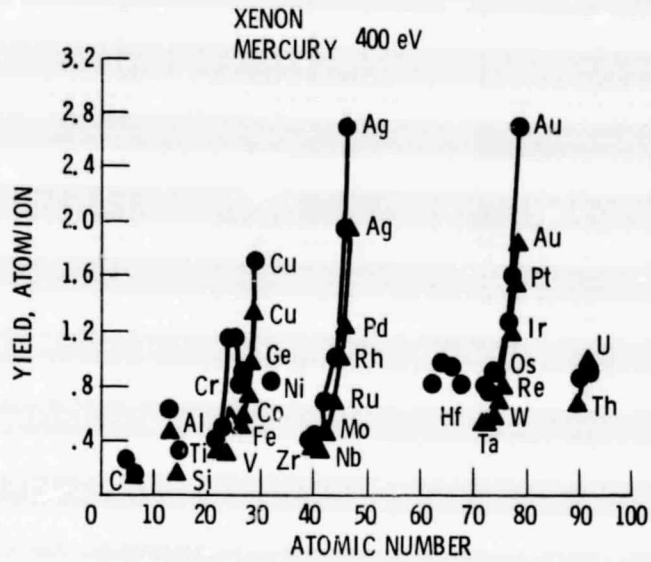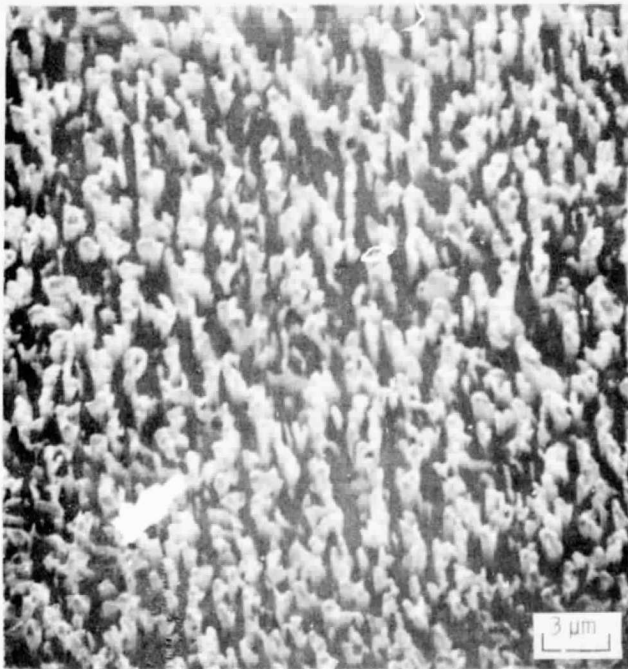
Figure 11. - Sputter yield versus atomic number of the substrate for low-energy ions, showing the periodicity effect (ref. 18).
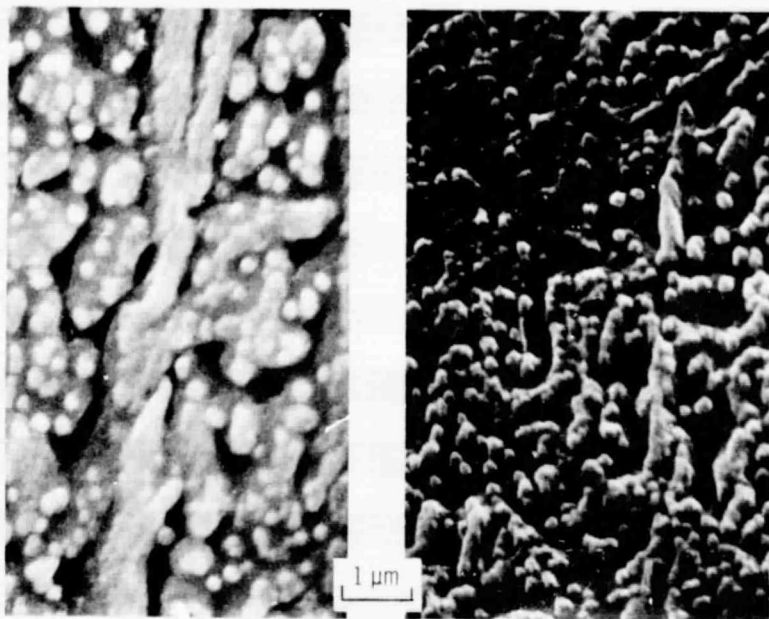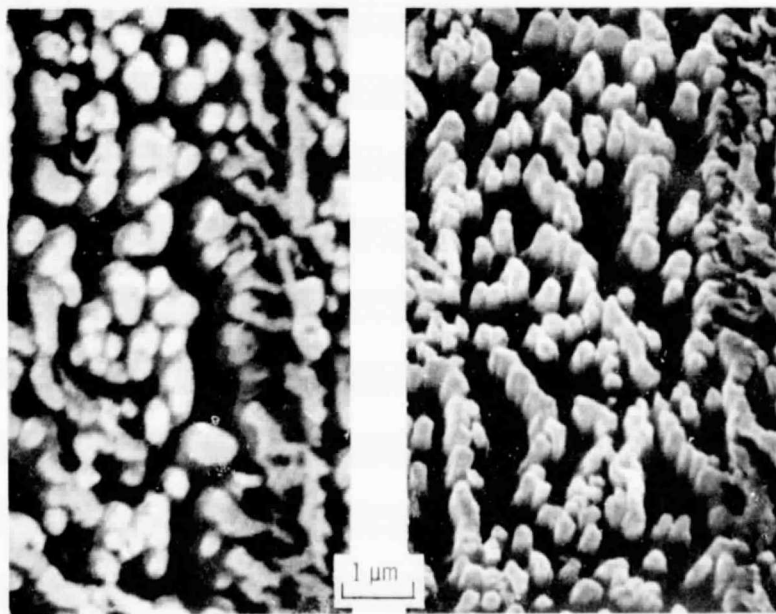
(a) NICKEL.

(b) COPPER.

Figure 12. – Scanning electron photomicrographs of ion beam textured surface with tantalum seed material. Net accelerating potential, 1000 volts; beam current, 100 ma. X3000, 40° tilt.

(a) 0^0 tilt.   (b) 40^0 tilt.

Figure 13. - Scanning electron photomicrographs of an ion beam textured copper surface (two minute exposure), with tantalum as the seed material. Net accelerating potential, 1000 volts; beam current, 100 ma. X10 000.

(a) 0^0 tilt.   (b) 40^0 tilt.

Figure 14. - Scanning electron photomicrographs of an ion beam textured copper surface (four minute exposure) with tantalum as the seed material. Net accelerating potential, 1000 volts; beam current, 100 ma. X10 000.
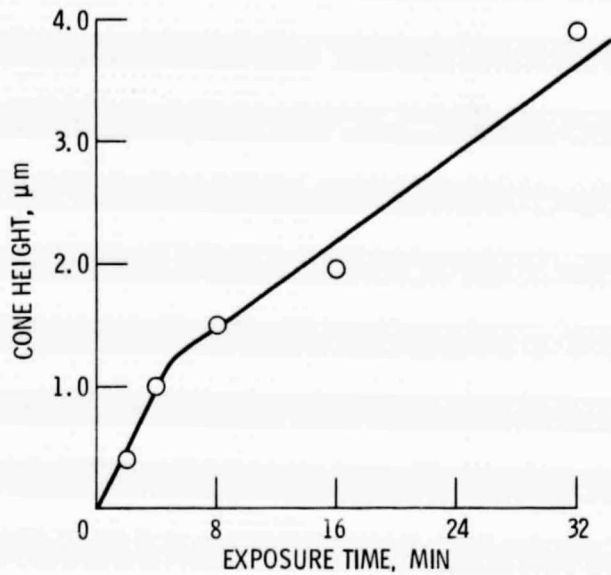
Figure 15. - Measurements of the copper cone
height with respect to ion beam exposure time.
Xenon ion beam operated at 1000 volts and
100 ma. Tantalum was the seed material.

(a) 40° tilt; X3000.

(b) 40° tilt; X1000.

Figure 16. - Scanning electron photomicrographs of ion beam textured
copper. (a) Tungsten seed material; (b) Al_2O_3 seed material. Net
accelerating potential, 1000 volts; beam current, 100 ma.